International Journal of Advanced Research in Chemical Science (IJARCS)
Volume 10, Issue 1, 2023, PP 1-13
ISSN No. (Online) 2349-0403
DOI: http://dx.doi.org/10.20431/2349-0403.1001001
www.arcjournals.org

Experimental and Computational Investigation of Anticorrosion Properties of Eastern Nigerian Propolis Extract on Mild Steel in Acidic Medium

Godwin Abawulo Ijuo[1*], Pius OziriUkoha[2], John Ogbaji Igoli[1]

[1]*Department of Chemistry, Federal University of Agriculture, PMB, 2373, Makurdi, Nigeria*
[2]*Department of Pure and Industrial Chemistry, University of Nigeria, Nsukka*

Corresponding Author:** ***Godwin Abawulo Ijuo, *Department of Chemistry, Federal University of Agriculture, PMB, 2373, Makurdi, Nigeria*

Abstract: *NMR and FTIR analyses were used to evaluate methanol extracts from Eastern Nigeria propolis. The main component of the extract was determined to be lupenone (LEU). Gravimetric, electrochemical impedance spectroscopy, and computational approaches were employed in the studies of the adsorptive and inhibitive effects of the propolis extracts on the corrosion of mild steel (MS) in 1.0 M HCl. The results showed that the inhibition efficiency reduced with rising temperature but rose with inhibitor concentration. Impedance analysis revealed that charge transfer alone was responsible for controlling the corrosion process. The double layer capacitance (Cdl) reduced as the concentration of the inhibitor rose, while the charge transfer resistance (R_2) increased.The activation energy and Gibbs free energy values point to a physical and spontaneous adsorption of the extract components on the MS surface. The Langmuir adsorption isotherm model was used to predict the adsorption of propolis extract onto the surface of the MS. Theoretical studies showed that the oxygen atom plays a major role in how LEU interacts with the MS. The electron cloud on the O atom of the C=O group, as well as the density throughout the C=C and C=O groups, are all depicted on the HUMO map. The LEU have Me2C= as the site for nucleophilic attack, whereas the C=O is the site for electrophilic assault, according to calculations using the fukui function indices. Results showed that propolis extracts successfully created a barrier effect on the MS corrosion in 1.0 M HCl.*

Keywords: *Propolis, Lupenone, Mild steel, Corrosion Inhibition, Adsorption, Density Functional Theory (DFT)*

1. INTRODUCTION

The performance of metallic materials in use is most negatively impacted by corrosion, a naturally occurring phenomenon. Due to its extensive use in both industrial and home settings, mild steel appears to be particularly susceptible to several types of corrosion [1]. Because mild steel is vulnerable to corrosion, proactive precautionary measures need to be established. One of the tried-and-true techniques for preventing and controlling corrosion that can lessen or completely eliminate its effects on the environment, economy, and public safety is the use of inhibitor [2].The estimated cost of corrosion in globally in 2013 was $2.5 trillion, equivalent of 3.4% of the world's GDP. Oil and gas companies loses an average of $765 million annually to corrosion in Nigeria alone.

Of this amount, chemical treatment gulps 81% of the entire cost while coating takes the balanced 19% cost of prevention. With respect to the contribution of corrosion maintenance methods, 60% goes for repairs while 40% for replacement. The estimated realizable savings on a global basis, of the cost of corrosion is about 35%, on the condition that available corrosion control practices are applied. This amounts to $875 billion, [3-4].The application of organic corrosion inhibitors like propolis extract will be useful in minimising loses caused by corrosion.

Chemical treatment consumes 81% of the whole cost of prevention, while coating accounting for the remaining 19% of this cost. Regarding the contribution of corrosion maintenance techniques, 60% is spent on repairs and 40% is spent on replacement. If known corrosion control techniques are used, it is projected that about 35% of the cost of corrosion, equivalent of $875 billion, may be saved globally [3–4]. Utilizing organic corrosion inhibitors, such as propolis extract, will go a long way toward reducing corrosion-related losses.

Propolisis a viscous substance prepared by honeybees from leaf buds and flowers. Sometimes known as "bee glue," to smooth out walls, plug fissures, manage temperature and moisture levels, and keep the hive environment aseptic all year round.

Due to its broad biological properties, including its antibacterial, antioxidant, anti-inflammatory, anticancer, anti-HIV, and antiulcer actions, propolis has recently piqued the interest of researchers [5]. It is frequently used to both prevent and treat conditions like the common cold, wounds, ulcers, rheumatism, sprains, heart disease, diabetes, and dental cavities. The plants from which the materials are collected, the season of collection, the location of the hive, the breeds of bees, and the period at which it was formed all affect the color and chemical content of propolis [6–8].Though honey comb waste still has a significant amount of flavonoids after they are being pressed to obtain honey, the propolis-containing honeycomb is thrashed into an organic waste that has no market value.

2. MATERIALS AND METHODS

The materials used include mortar and pestle, desiccator, NMR machine, Fourier Transform Infrared Spectrophotometer (FTIR), digital weighing balance, thermostated water bath and potentiostat. Other materials include mild steel, bristle brush and silicon carbide abrasive paper (#600-# 1200). Also used are two necked reaction flask, thermometer, measuring cylinders, beakers and routine laboratory apparatus. The reagents were of analar grade with re-distillation of the solvents; n-hexane, ethyl acetate and methanol. Hydrochloric acid solution was used as aggressive environment, acetone as drying agent, sodium hydroxide and ethanol for cleaning and degrease respectively. Preparation of the reagents were carried out using double distilled water.

2.1. Preparation and Extraction of Propolis Samples

Propolis samples were bought from bee farmer in Enugu, Eastern Nigeria. The samples were air dried for two weeks, and then pounded with a pestle and mortar. The fine powdered samples (100 g) were first defatted with n-hexane at room temperature by macerating for 72 h. This was followed by filtration with Whitman filter paper No. 1 using a vacuum pump. Following the same procedure, the residue were re-extracted with ethyl acetate and methanol, respectively. The solvents were completely removed using a rotary vacuum evaporator. The powdery extracts were then kept in dark bottles at 4 °C until use. A portion was taken from the concentrated extract for column chromatography and TLC to further separate and purify the extracts for NMR analysis.

2.2. ^{1}H NMR Analysis of the Propolis Extracts

Nuclear Magnetic Resonance (NMR) spectroscopic analysis on fractions of the propolis were analyzed using a Bruker-Avance 400 MHz) spectrophotometer with deuterated chloroform as solvent. The software Mestrenova 12 was used to analyze the NMR data. The compounds' 1H was compared with some chosen literatures to determine their characteristics and reveal their structures.

2.3. Corrosion Inhibition Experiments

2.31. Gravimetric Measurement

Mild steel coupons that had already been cleaned and weighed were submerged in 1.0 M HCl for 24 hours in order to evaluate the impact of propolis extract concentration on corrosion of mild steel. This was done at room temperature with and without 200-1000 ppm propolis extract. The weight loss was taken to be the difference between the weights of the coupon before and after the immersion period. The coupons were retrieved at 24 hours intervals for 7 days at room temperature, washed with distilled water and acetone, dried, and reweighed in order to determine the effect of time on the rate of mild steel corrosion. All test were carried out in duplicate. From the weight loss results, the inhibition efficiency (%IE) of the inhibitor and corrosion rate of mild steel were calculated using equation 1-2[10].

$$IE_{\exp} = \left(1 - \frac{W_{(1)}}{W_{(0)}}\right) x100 \qquad 1$$

where, $W_{(0)}$ is the weight loss of the mild steel without inhibitor and $W_{(1)}$ is the weight loss of mild steel with inhibitor.

$$CR\left(gh^{-1}cm^{-2}\right)=\frac{\Delta W}{At} \quad 2$$

where ΔW is the weight loss, A is the area of the coupon and t is the immersion time.

2.4. Electrochemical Impedance Spectroscopy (EIS) Measurements

The experiments were conducted at 303 K using 200 mL of test solution. A conventional three-electrode system consisting of MS as working electrode, an auxiliary electrode and a reference electrode were used for the measurements. The %IE were calculated from the charge transfer resistance (R_{ct}) values by using the equation

$$\%\text{IE}=\frac{\text{R}_{\text{ct}}-R_{ct}^{0}}{\text{R}_{\text{ct}}}\times 100 \quad 3$$

where, R_{ct}^{0} is the charge transfer resistance of MS without inhibitor and R_{ct} is the charge transfer resistance of MS with inhibitor. The double layer capacitance (C_{dl}) was calculated using equation 4

$$C_{dl}=\frac{1}{2\pi f_{max}\ R_{ct}} \quad 4$$

where f_{max} is the frequency at which the imaginary component of impedance is maximum.

3. Quantum Chemical Calculation

Full geometric optimization was carried out using ab initio and DFT level of theories in the Hyper Chem release 8.0 software. Semi-empirical parameters were calculated in different Hamiltonians: CNDO, MNDO and INDO: AM1 (Austin Model 1), PM3 (Parametric Method 3), using optimized structure of the studied inhibitor as an input to the software Windows. Calculations were performed on compatible laptop computer. The following quantum chemical indices were calculated: the Energy of the Highest Occupied Molecular Orbital (E_{HOMO}), the Energy of the Lowest Unoccupied Molecular Orbital (E_{LUMO}), the binding energy (E_b), the electronic energy (E_{elect}), the core repulsion energy E_{CCR}, the dipole moment (μ), the heat of formation (H_f) and the total energy of the molecule (E_T).

4. Results and Discussion

4.1. ^{1}H NMR Analysis

The most interesting characteristic signals obtained from the ^{1}H NMR spectrum (Figure 1) of the propolis sample include 4.57 (m, H29), 4.69 (m, H29) and the absence of H-3 at 3.20 ppm. Comparing the data with literature, *Lupenone* (LUP) shown as Figure 1was the identifiable compound present in ENPE [11]. LUP is aterpenoids, specifically a triterpenoid. It belongs to lupane type triterpenoids. Terpenoids are one of the largest and diverse groups of phytochemicals. They are known class of phytochemicals with functional groups that are active inhibitor of corrosion due to the presence of heteroatoms in the compound. They usually contain 30 carbon atoms consisting of 6 isoprene units. Their effectiveness as corrosion inhibitors is attributed to the presence of active sites that can be converted into other big class of compounds such as saponins, [12-13].

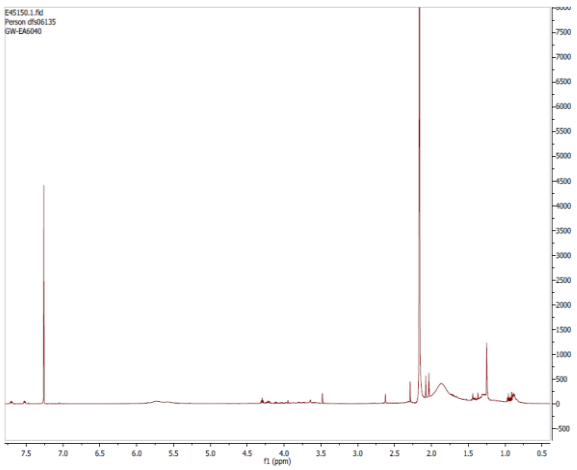

Figure1. *Proton NMR spectrum of ENPE*

4.2. FTIR Study

FTIR analysis of the ENPE was carried out in order to ascertain the functional groups present in the sample. **Figure 2** shows the spectrum of both the raw ENPE and the corrosion product. The important peaks are recorded in **Table 1.**

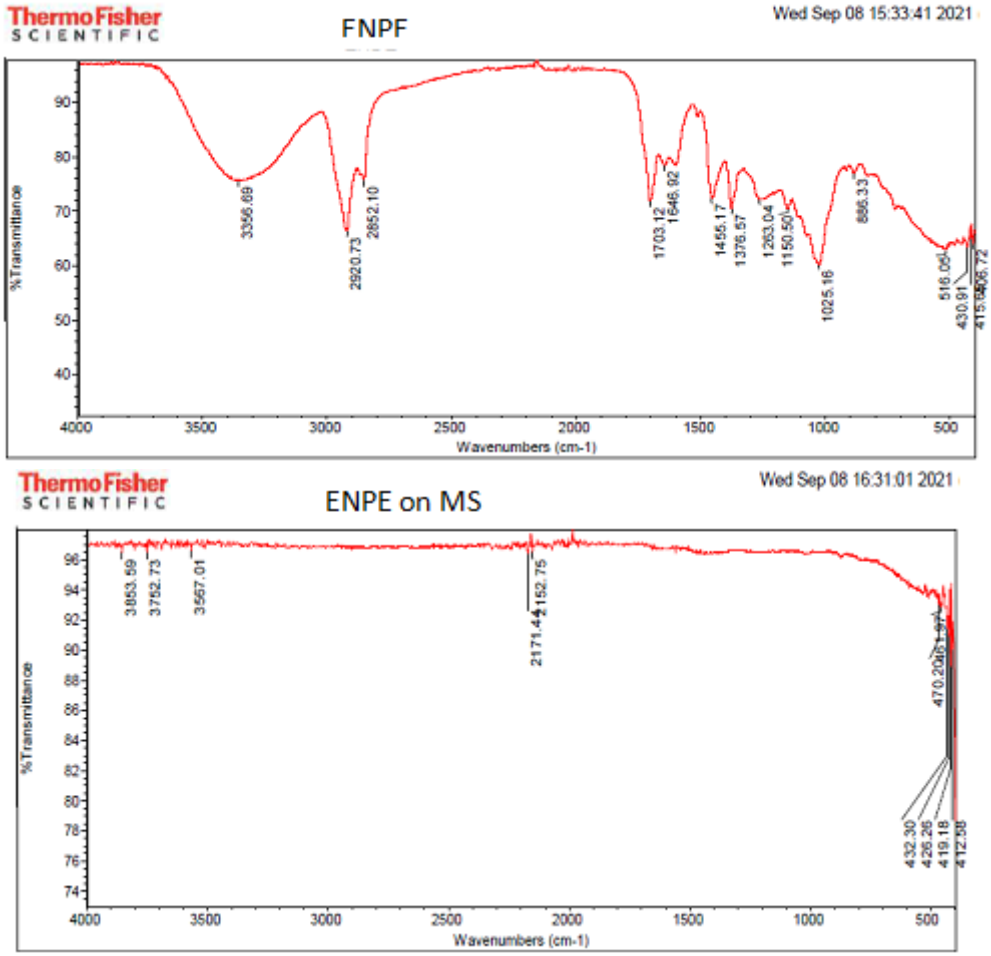

Figure2. *FTIR spectrum of ENPE and the corrosion product of the mild steel in the presence of ENPE*

Table 1. *Frequencies and peak intensities of FTIR absorption by ENPE and that of the corrosion product*

ENPE before adsorption		**Corrosion product in the presence of ENPE**		**Functional group/assignment**
Frequency (cm^{-1})	**Intensity**	**Frequency (cm^{-1})**	**Intensity**	
3356.69	Broad, strong	3567.01	weak	O-H stretching
2920.73	strong			O-H stretching
2852.10	medium			C-H stretching
1703.12	strong			C=O stretching
1646.92	medium			C=N imine
1455.17	medium			C-H bending, alkanes
1376.57	medium			O-H Alcohol
1263.04				C-O stretching
1150.50	strong			C-O stretching tertiary alcohol
1025.16	strong			C-N stretching
863.33	weak			C=C bending

The broad and strong intensitiesat peaks ranging from 3356.69 cm^{-1} to 2920.73 $cm^{-1}$are due to O-H group, 2852.10 cm^{-1} correspond to alkyl C-H stretching, 1703.12 cm^{-1} is assigned C=Ostretching, 1646.92 $cm^{-1}$is attributed to C=N imine, 1455.17 cm^{-1} is assigned C-H bending of alkane, the 1376.57 cm^{-1} is assigned O-H of alcohol. The peak at 1263.04$cm^{-1}$is attributed to C-O stretching of tertiary alcohol, 1025.6 $cm^{-1}$is assigned C-N stretching,while the peak at 863.33$cm^{-1}$is assigned C=C bending.

It can be seen that functional groups not part of LUP were identified by FTIR analysis. This implies the possibility of the presence of compounds other than LUP in the propolis sample used.

4.3. Corrosion Inhibition Studies

4.3.1. Gravimetric Measurements

Table 2 present the inhibition efficiencies of ENPE on mild steel in 1.0 M HCl calculated from equation 1. The result show that the inhibition efficiencies increased with increase in concentration of the inhibitor.The corrosion rates (**Figure 3a)** were found to decrease with increase in concentration of ENPE but increase with time.The inhibition efficiencies increased with increase in concentration of ENPE. This behaviour could be attributed to the increase in adsorption of inhibitor on the metal or at the solution interface on increasing its concentration[14].

Table 2. *Inhibition efficiencies of the various inhibitors on mild steel in 1.0 M HCl*

Time (hrs)	ENPE Concentration (ppm)					
	Blank	**200**	**400**	**600**	**800**	**1000**
24	-	67.35	69.63	71.79	73.18	76.82
48	-	69.79	71.60	74.48	76.21	76.94
72	-	70.40	72.77	73.00	75.44	77.11
96	-	80.48	80.78	83.03	85.43	85.91
120	-	84.08	86.10	87.42	89.71	93.94
144	-	85.50	86.58	88.63	89.87	95.10
168	-	82.11	84.74	85.03	87.98	95.31

4.3.2. Effect of Temperature

Table 3 provides a summary of the values for ENPE inhibition efficiency on mild steel in 1.0 M HCl based on the impacts of temperature at 303, 313, 323, 333, and 343 K. Although the magnitude of the inhibition efficiencies varies, the results from the effect of temperature are generally less favorable than those from the weight loss method. Inhibition efficiencies rise with an increase in ENPE concentration, following a similar pattern to those found in weight loss method results. However, as the temperature rose, the effectiveness of the inhibition reduced. Additionally, it was discovered that corrosion rates (**Figure 3b**) rose with temperature. This is another proof that ENPE effectively prevents mild steel from corroding in hydrochloric acid.The physical adsorption of ENPE to the surface of mild steel is responsible for the decrease in inhibitory effectiveness with rising temperature. According to reports, chemisorption is preferred at higher temperatures, but physical adsorption is preferred at lower temperatures, [15].

Table 3. *Inhibition Efficiencies of ENPE on Mild Steel in 1.0 M HCl at 303 – 343 K*

Temperature (K)	Inhibitor Concentration (ppm)					
	Blank	**200**	**400**	**600**	**800**	**1000**
303	-	56.16	62.47	77.42	80.77	91.23
313	-	52.32	59.52	61.12	71.67	79.62
323	-	49.54	46.06	53.09	62.43	67.17
333	-	32.51	39.12	40.32	51.34	55.12
343	-	32.13	36.12	36.87	40.67	43.07

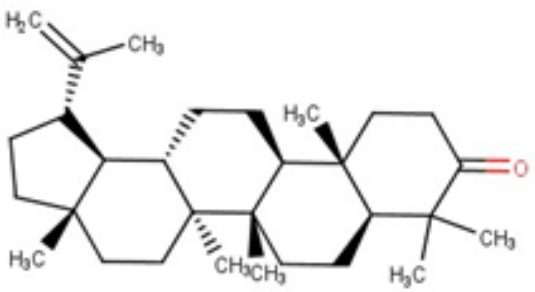

Figure 3. *Structure of lupe none elucidated from ENPE*

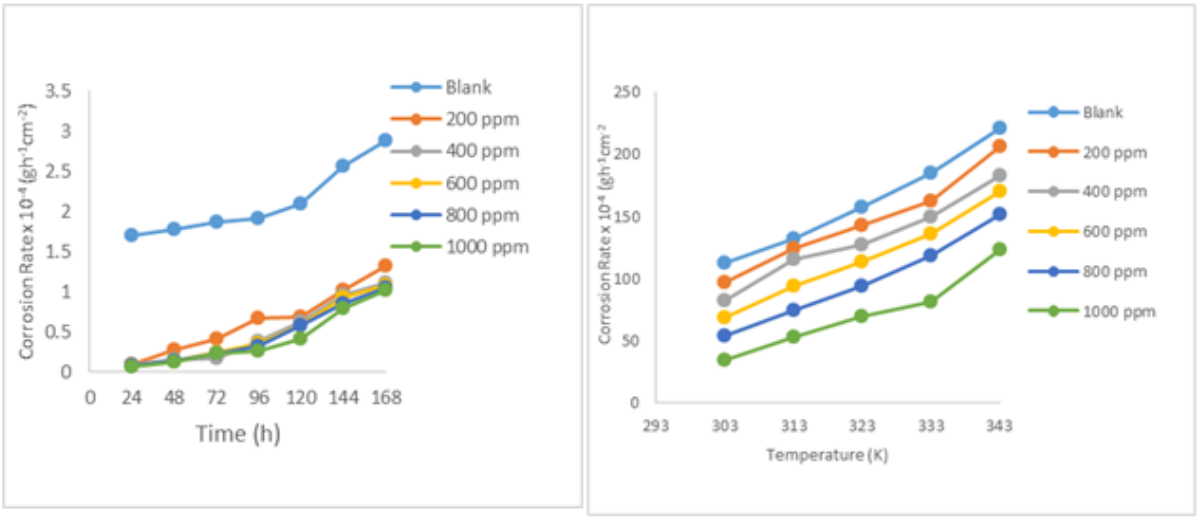

Figure 4. *Corrosion rates of mild steel in 1.0 M HCl in the absence and presence of the various concentration of ENPE as* ***(a)*** *a function of immersion time (h)* ***(b)*** *a function of temperature (K)*

4.4. Electrochemical Measurements

In order to ascertain the kinetic parameters for electron transfer reactions at the steel/electrolyte interface and concurrently addressing the surface characteristics of the examined system, electrochemical impedance spectroscopy (EIS) measurements at open-circuit potential were performed. Based on the shape of the Nyquist plots, the impedance data was analyzed using a best fit equivalent circuit. In order to fit the Nyquist plot in the absence and presence of an inhibitor in a solution of 1.0 M hydrochloric acid, the simplest Randles equivalent circuit (Figure 4) was used. It consists of one constant phase element, the fast charge transfer process R_1, the surface layer resistance R_2, and (CPE). By adding R_1 and R_2 at various inhibitor doses, the polarization resistance R_p, which is comparable to charge transfer resistance R_{ct}, was obtained. The % inhibition efficiency from equation 3 was then calculated using the resulting R_{ct}. Additionally, using equation 4, the double layer capacitance (Cdl) was computed. The charge transfer resistance (R_{ct}), constant phase element (CPE), and inhibitory efficiency are the parameters acquired from the measurement of EIS, as indicated in Table 4.The impedance diagram produces a single shape of depressed semicircle. This indicates that the corrosion process is brought on by charge transfer. Without the inhibitor, the modulus of the Nyquist plots in 1.0 M HCl solution was significantly lower than that in the presence of the inhibitors. The Nyquist plot reveals that increasing the concentration of inhibitor causes an increase in both the diameter of the semicircles and R_{ct} values, this is due to increase in the number of absorbed inhibitor molecules on the surface of the mild steel with increase in concentration. This also implies an increase in the corrosion inhibition efficiency The higher the resistance value (Rct), the smaller the electrical current I flow, and the fewer electrons are transmitted across the metal surface, according to the ohmic equation, which states that V = iR. Mild steel's cathodic oxidation is so prevented. The semicircles' identical shapes in both the absence and presence of the inhibitors point to a similar corrosion mechanism regardless of the inhibitors' presence.

The frequency dispersion of interfacial impedance is a phenomena that results in the Nyquist diagrams (**Figure 5a**) not being exact semicircles. Due to the presence of a non-ideal frequency response for which constant phase element CPE was utilized, this is caused by the surface roughness or inhomogeneity of the metal surface connected with solid metal electrodes [17].

The Bode impedance and Bode phase charts for the mild steel electrode in the presenceand absence of ENPE in 1.0 M HCl solution are shown in **Figures 5 (b and c**), respectively. It is clear that the Bode plot only contains a single capacitive loop. Bode phase plot showed that larger negative values of phase angle at the intermediate frequency were produced by an increase in inhibitor concentration. The measurements of phase angle became increasingly negative as the inhibitor's concentration rose. This shows that more inhibitor molecules are adsorbed at the mild steel surface, which is why the inhibitive behavior happened [18].

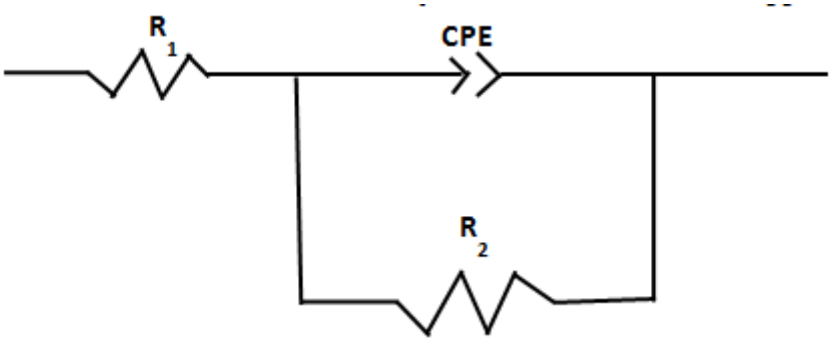

Figure 5. *Equivalent circuits used to fit experimental EIS data for the corrosion of the mild steel in 1.0 M hydrochloric acid solution in the absence and presence of the inhibitor*

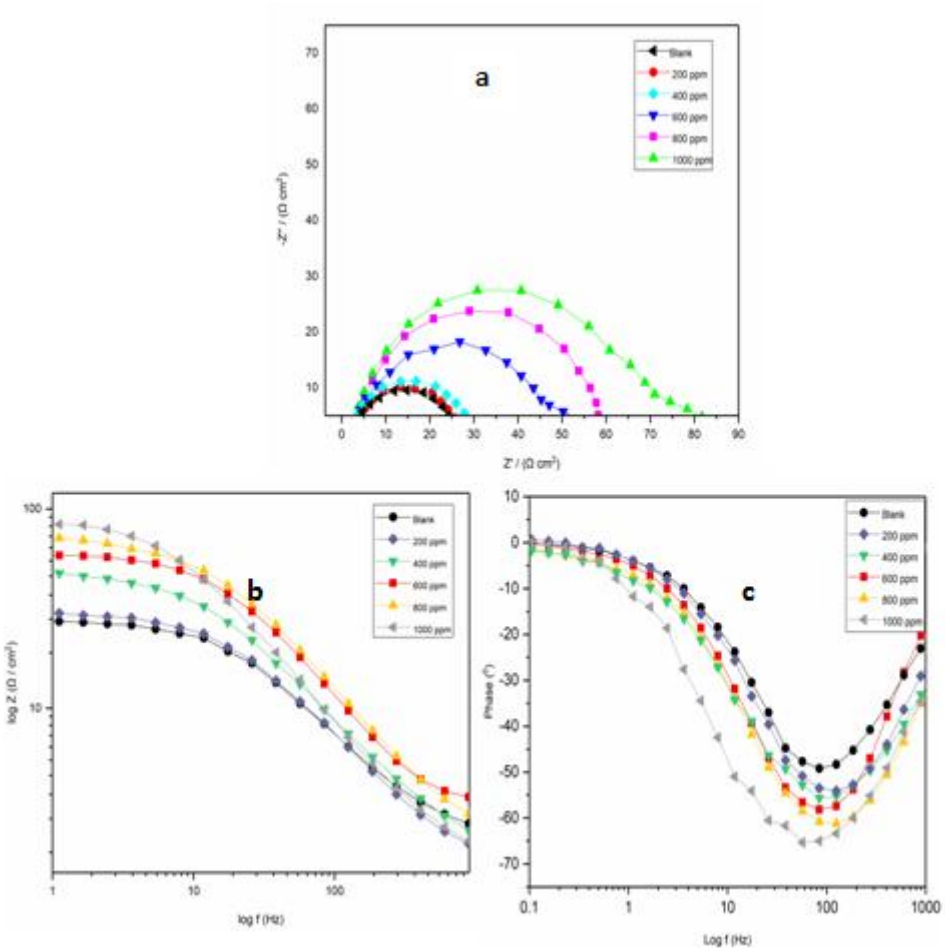

Figure 5. ***(a)*** *Nyquist plots* ***(b)*** *Bode impedance and* ***(c)*** *Bode phase plots for the mild steel specimen in 1.0 M HClin the absence and presence of different concentrations of ENPE*

Table 4. *Impedance parameters for the corrosion of mild steel in 1.0 M HCl in the absence and presence of various concentrations of the inhibitors*

Inhibitor	Concentration (ppm)	R_1(Ω cm^2)	R_2(Ω cm^2)	R_{ct}(Ω cm^2)	C_{dl} (µFcm^{-2})	n	%IE
ENPE	Blank	1.205	10.414	11.619	9.34×10^{-4}	0.88	-
	200	3.566	29.595	33.161	2.74×10^{-4}	0.87	64.96
	400	5.583	53.442	59.025	2.40×10^{-4}	0.84	80.31
	600	9.874	59.491	69.365	2.02×10^{-4}	0.91	83.25
	800	17.096	81.447	98.543	2.15×10^{-5}	0.83	88.21
	1000	29.157	89.897	119.054	1.58×10^{-5}	0.87	90.24

4.5. Thermodynamic Consideration

The thermodynamic behaviour of ENPE was critically studied in order to gain insight into the mechanism of inhibition of the corrosion of mild steel in 1.0 M HCl by ENPE. Thermodynamic parameters such as the energy of activation (Ea), standard enthalpy (ΔH) and the entropy changes of adsorption (ΔS), were deduced through the transition state plots. The transition state equation 5 relates the corrosion rate with these thermodynamic parameters, which was further resolved to a linear expression of equation 6.

$$CR = \frac{RT}{Nh}\exp^{\left(\frac{\Delta S_{ads}}{R}\right)}\exp^{\left(\frac{-\Delta H_{ads}}{RT}\right)} \quad 5$$

$$\log\left(\frac{CR}{T}\right) = \log\left(\frac{R}{Nh}\right) + \left(\frac{\Delta S_{ads}}{2.303R}\right) - \left(\frac{\Delta H_{ads}}{2.303RT}\right) \quad 6$$

The Arrhenius plot for the corrosion of mild steel in 1.0 M HCl containing various inhibitor concentrations is shown in **Figure 6a**. The calculated parameters are listed in Table 5. The table shows that the values for the activation energy are larger when ENPE is present than when it is not. With an increase in inhibitor concentration, the Ea values likewise went up. The corrosion of mild steel in a blank solution of 1.0 M HCl was measured to have an Ea of 14.68 $Jmol^{-1}$. This value increased with increasing inhibitor concentrations, reaching its highest value of 34.41 $Jmol^{-1}$ in the presence of 1000 ppm ENPE.

This demonstrated that the adsorbed inhibitor had created a physical barrier to the mass transfer and change, which had reduced the rate of corrosion [19]. According to a previous publication, physical adsorption is implied by a value of Ea less than 80 kJ mol^{-1} and chemical adsorption by a value of Ea larger than 80 kJ mol-1 [20]. ENPE was physically adsorbed on the coupons, as shown by the experimentally measured Ea values, which are all less than 80 kJ mol^{-1}. It is possible that a multilayer protective coating on the entire surface of mild steel was attained.

Figure 6b displays the transition state plots for the corrosion of mild steel in 1.0 M HCl in both the absence and presence of ENPE. Table 6 contains the corresponding transition state parameters, such as ΔH and ΔS, deduced from the plot of ln $(\frac{CR}{T})$vs $\frac{1}{T}$. The table shows that the values of ΔS are negative and gradually decrease with increasing inhibitor concentration, indicating ordered fashioned adsorption of the freely flowing inhibitor molecules in the bulk solution onto the mild steel surface. This suggests that the reaction was both spontaneous and possible, and that the activation complex comprises association stages. Additionally, studies revealed that all of the ΔH values are negative, confirming their exothermic nature of the mild steel dissolution process [21].

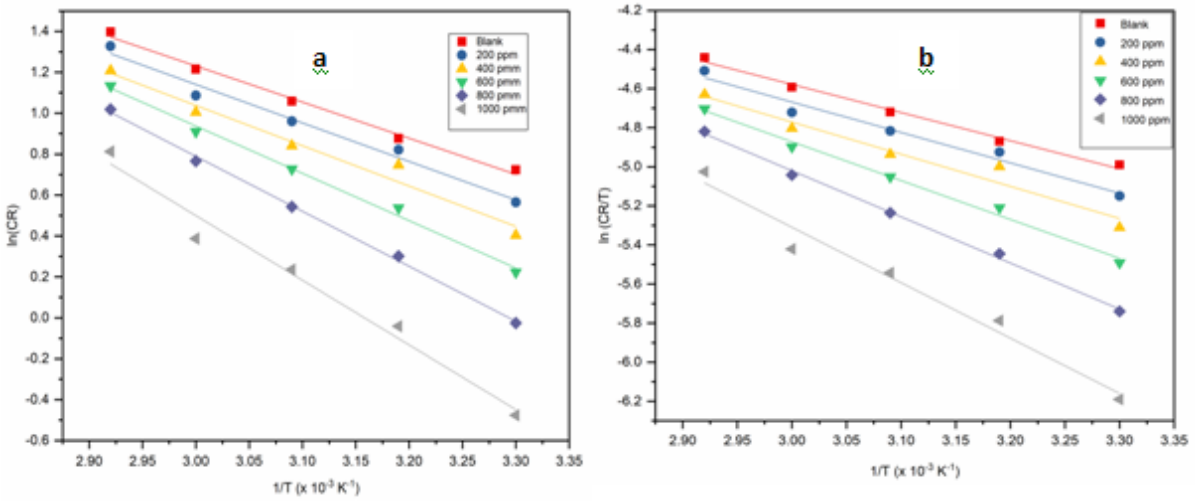

Figure 6. ***(a)*** *Arrhenius and* ***(b)*** *Transition state plot for the corrosion of mild steel in 1.0 M HCl containing the various concentration of ENPE*

Table 5. *Thermodynamic and adsorption parameters for the corrosion of mild steel in 1.0 M HCl containing various concentration of ENPE*

Concentration (ppm)	ENPE					
	Ea (J/mol)	ΔS^0_{ads} (J/mol)	ΔH^0_{ads} (J/mol)	R^2	k_{ads}	ΔG^0_{ads} (kJ/mol)
Blank	14.68	-199.68	-11.97	0.99		
200	15.65	-197.51	-12.95	0.98	0.1398	-5.16
400	16.39	-196.17	-13.68	0.97	0.2438	-6.78
600	19.24	-188.45	-16.53	0.99	0.3935	-8.28
800	22.34	-180.36	-19.64	0.99	0.2031	-6.71
1000	26.28	-170.95	-23.58	0.97	0.7159	-10.50

4.6. Adsorption Consideration

Adsorption isotherm values are crucial for explaining the mechanism of corrosion inhibition potentials of metal and alloy organo-electrochemical processes. Adsorption isotherms are depicted in general form by Equation 7. To learn more about the interaction between the mild steel surface and ENPE at various temperatures, various adsorption isotherms were explored. It was determined that the Langmuir adsorption isotherm provided the best fit, in which case the linear regression coefficients (R^2) were nearly one. According to the Langmuir adsorption isotherm, each adsorption site on a solid surface has a fixed quantity of adsorbed species present, [22].

$$f(\theta, x)\exp^{(-2a\theta)} = KC \qquad 7$$

The Langmuir isotherm plots of log C/θ against log C for the adsorption of ENPE at various temperature is shown as **Figure 7**. Equation 8 shows the relationship between the equilibrium constant of adsorption of the inhibitors on the mild steel surface and the standard free energy of adsorption ΔG^0_{ads}

$$\Delta G^0 ads = -2.303RT \log (55.5Kads) \qquad 8$$

Where Ris the molar gas constant, T is the absolute temperature, and 55.5 is the water concentration in solution expressed in mol L^{-1}. Langmuir parameters ($\mathbf{k_{ads}}$and$\mathbf{\Delta G^0_{ads}}$)for the corrosion of mild steel in 1.0 HCl containing various concentrations of ENPE calculated from the slope and intercept of the plots are recorded as part of **Table 5**.All the values obtained for in the ΔG were negative indicating that the adsorption process proceeded spontaneously and confirms physical adsorption mechanism. Generally, the value of ΔG°ads ≤ −40 kJ mol^{-1} signifies physisorption and values more negative than −40 kJ mol^{-1} signify chemisorption [23].

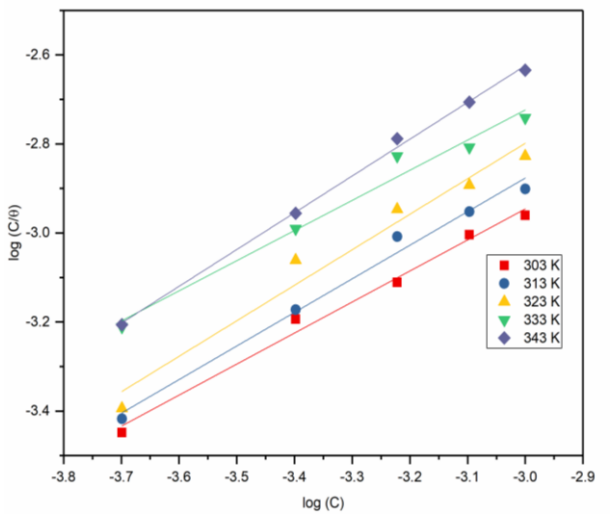

Figure 7. *Langmuir isotherm for the adsorption of ENPE on mild steel surface in 1.0 M HClsolution at various temperature*

4.7. FTIR Analysis

Figure 2 shows the infrared spectra of raw ENPE and that of ENPE adsorbed on the MS surface. Almost all the peaks **(Table 1)** which appeared in the raw extract are no longer visible in the corrosion product. The only visible peak which was strong at 3567.01 in the raw sample became weak in the corrosion product. This is indicative of the fact that atoms contained in ENPE have actively participated in the adsorption process, forming metal complexes that are active against corrosion reactions.

4.8. DFT Calculations on Corrosion Inhibition Potential of the Compounds

In order to understand the electron distribution of the inhibitor at the molecular level and the nature of its interactions with the metal surfaces, quantum chemical simulations were carried out. LUP, the identified organic molecule (**Figure 3**), was investigated for potential use as a corrosion inhibitor. The 3-dimensional structure of the compound (**Figure 8a**) was retrieved from the PubChem database for chemical molecules [24]. Chem3D Ultra 10.0 application [25] was used to convert the molecules from their 3D representations to a 2D version (Figure SM5) for a clearer view of the structures.

For the purpose of seeing calculation setups and outputs, the Gauss View 6.0 application [26] was used. All computations were performed using the widely used density functional theory (DFT) model incorporated in Gaussian 16 [27]. The model for all calculations was the hybrid density B3LYP functional [28] with the 6-31+G(d,p) basis set. The calculations performed include computations for ultraviolet (UV-Vis) radiation, frequency optimization, and geometry optimization. First in the gas phase, then in the experimental solvent, HCl, geometry optimization was done. The starting structures for the two following calculations were the molecules' optimized geometries from geometry optimization.

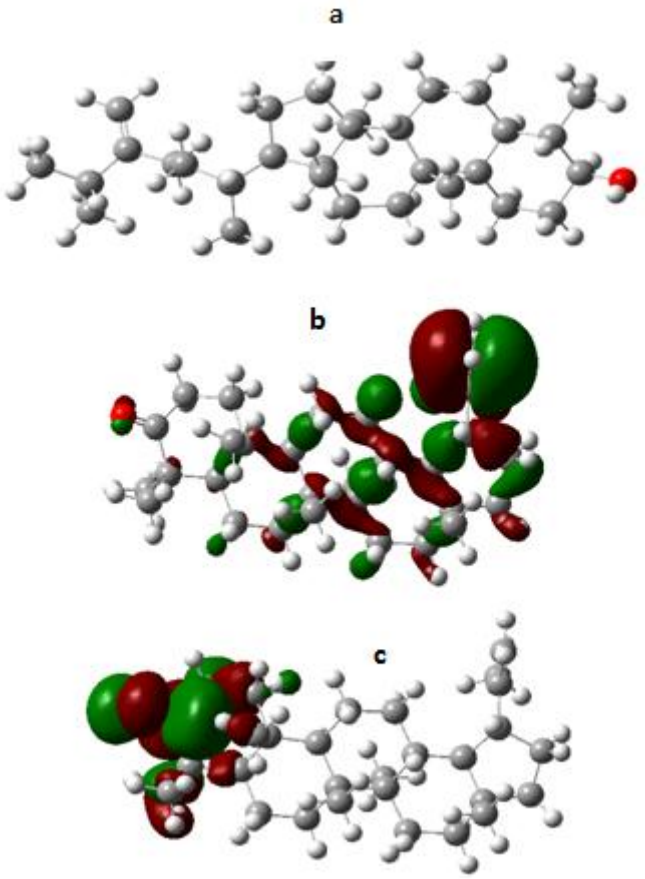

Figure 6. *(**a**) 3D structures of Lupenone(**b**) The (HUMO) Density (**c**) The (LUMO) of LUP using DFT at the B3LYP/6-31G(d,p) Basis Set Level.*

Each compound's neutral (zero charge and singlet spin), cationic (+1 charge and doublet spin), and anionic (-1 charge and doublet spin) molecules underwent little frequency optimization. These allow

for the calculation of the atomic population charges, the fukui function, and a further evaluation of potential corrosion inhibition centers. In order to determine the molecular orbital energies for further analysis of the energy gap and other electronic parameters, UV-Vis calculations involve single-point energy calculations.

Table6. *Electronic properties and global reactivity descriptors for LUP*

E_{LUMO} (eV)	E_{HOMO} (eV)	ΔE (eV)	A (eV)	I (eV)	η (eV)	δ (eV^{-1})	χ (eV)	C_p (eV)	ω (eV)	ΔN	μ (Debye)
-0.82	-6.54	5.72	6.54	0.82	2.86	0.34	3.68	-3.68	2.37	0.57	4.98

Every single optimized structure has a positive vibration frequency and is a valid local minimum. The single-point energy calculation was used to calculate the energies of the molecular orbitals, which include the lowest unoccupied molecular orbital, ELUMO (Figure 6A), and the highest occupied molecule orbital, EHOMO (Figure 6B) (Table SM3). The energy gap (E) is determined by the difference between these two values. The ability of molecules to bind and interact with one another is measured by chemical hardness. The intermolecular reactivity sequence of any given chemical or collection of compounds can be constructed using this index as a guide [29]. Low values of, which imply soft and robust intermolecular reactivity, were obtained with correspondingly high values of for LUP. A molecule will contribute electrons to any interacting species if its ΔN value is larger than zero, according to research [30–31]. LUP will donate a significant amount of electrons and hence function as effective inhibitors because the ΔN values are very near to 1, with a decent inhibitory potential of 0.57.

Typically, LUP is made up of three atoms: oxygen, carbon, and hydrogen. The electronegative carbonyl oxygen atom at a rare end of the molecule in comparison to the numerous aliphatic groups in the molecule may be the cause of the polarity in LUP, which makes it an effective corrosion inhibitor.

4.9. Molecular Orbital and Fukui Index Analysis

The electron cloud on the O atom of the C=O group is visible on the HOMO map in LUP. It is also distributed densely over the C=C and C=O groups and partially across two cyclohexanes. It's interesting to note that several of the functional groups that account for the HOMO are also seen to support the molecules' molecular reactivity. LUP has the $Me_2C=$ as the site for nucleophilic attack and the C=O as the site for electrophilic attack based on calculations of the Fukui function indices. The outcomes have shown that the LUP molecule can prevent steel metal surfaces from corroding in an acidic media like HCl.

5. CONCLUSIONS

ENPE has shown to be an effective inhibitor of mild steel corrosion in HCl. The % IE was found to rise with higher inhibitor concentrations but fall with higher temperatures. The results from gravimetric, electrochemical, and computational methods are well-aligned. The activation complex is thought to reflect association stages and that the reaction was spontaneous and feasible based on the negative values of entropy changes of adsorption (ΔS). The values of ΔG^0_{ads} supported the spontaneity. Additionally, the inhibitors' enthalpies of activation (ΔH) are all negative, suggesting the exothermic nature of the mild steel dissolution process in HCl, according to the data.The physically adsorbed ENPE on the mild steel surface in HCl was determined to obey the Langmuir adsorption isotherm based on the value of the activation energy (EA), standard free energy of adsorption ΔG^0_{ads}, and adsorption isotherms. LUP uses the Me2C= as the nucleophilic attack site while using the C=O as the electrophilic attack site. Because of its capacity to donate a sizable number of electrons, it functions well as an inhibitor.

ACKNOWLEDGEMENT

The authors extend their appreciation to the Department of Chemistry, University of Agriculture Makurdi and the Department of Pure and Industrial Chemistry, University of Nigeria, Nsukka for granting us access to their laboratories and equipment respectively.

REFERENCES

[1] D. Zhang, H. Zhang, S. Zhao, Z. Li, S. Hou "Electrochemical Impedance Spectroscopy Evaluation of Corrosion Protection of X65 Carbon Steel by Halloysite Nanotube-Filled Epoxy Composite Coatings in 3.5% NaCl Solution" Int. J. Electrochem. Sci., 14 (2019), 4659 – 4667, doi: 10.20964/2019.05.09

[2] B.R. Fazal, T. Becker, B. Kinsella and K. Lepkova "A review of plant extracts as green corrosion inhibitors for CO2 corrosion of carbon steel" npj Materials Degradation 5 (2022), doi.org/10.1038/s41529-021-00201-5

[3] D.C. Benjamin, A.L. Richard, H.R. David, "Corrosion control and monitoring; a program management guide for selecting materials", Advanced Materials, Manufacturing and Testing Information Analysis Center (AMMTIAC), New York, USA, (2006) 1-19.

[4] G.A. Ijuo, S. Nguamo, J.O. Igoli, "Ag-nanoparticles Mediated by Lonchocarpuslaxiflorus Stem Bark Extract as Anticorrosion Additive for Mild Steel in 1.0 M HCl Solution", Prog. Chem. Biochem. Res. 5(2022) 133-146, DOI: 10.22034/pcbr.2022.324366.1208

[5] A.K. Kuropatnicki, E. Szliszka, W. Krol, "Historical aspects of propolis research in modern times.Evid.Based Complement.Alternat. Med. 2013(2013) doi.org/10.1155/2013/964149

[6] E.V. Starostensko, "Propolization by bees of various races", Pchelovodsvo, 88 (1968) 30

[7] V.D. Wagh "Propolis, a wonder bees product and its pharmacological potentials" Adv Pharmacol Sci308249:(2013)

[8] G.A. Burdock, "Review of the biological properties and toxicity of bee propolis" Food and Chemical Toxicology; 36(1998) 347–363

[9] S. Patil, N. Desai, K. Mahadik, A. Paradkar, "can green synthesized propolis loaded silver nanoparticulate gel enhance wound healing caused by burns?" European Journal of Integrative Medicine S1876-3820(2015)00043-8 http://dx.doi.org/10.1016/j.eujim.2015.03.002

[10] H.F.Chahul, C.O. Akalezi, A.M. Ayuba, "Effect of adenine, guanine and hypoxanthine on the corrosion of mild steel in H3PO4'', International Journal of Chemical Science, 7(2015), 2006-3350

[11] C.V.S. Prakash and IndraPrakash, "Isoliation and Structural Characterisation of LupaneTritepenes from Polypodium Vulgare", Research Journal of Pharmaceutical Sciences 1(2012), 23-27

[12] P. Shagufta, "Terpenes and Terpenoids", Chapter 1, ISBN 978-953-51-6013-7

[13] N. Bhardwaj, P. Sharma and V. Kumar, "Phytochemicals as steel corrosion inhibitor: an insight into mechanism" Corros Rev; 39(2021), 27–41, doi.org/10.1515/corrrev-2020-0046 R

[14] W.A.W. Elyn, "Corrosion inhibition of mild steel in 1 M HCl solution by XylopiaFerruginea leaves from different extract and partitions", Int. J. Electrochem. Sci. 6 (2011) 2998-3016.

[15] G.A. Ijuo, A.M. Orokpo, P.N. Tor, "Effect of Spondiasmombin Extract on the Corrosion of Mild Steel in Acid Media", Chemrj, 3 (2018) 64-77

[16] E. Ituen, A. Singh, L. Yuanhua and O. Akaranta, "Green synthesis and anticorrosion effect of Allium cepa peels extract-silver nanoparticles composite in simulated oilfield pickling solution" SN Appl. Sci. 3 (2021) 679. https://doi.org/10.1007/s42452-021-04670-w

[17] N. B. Iroha, N. J. Maduelosi, "Corrosion Inhibitive Action and Adsorption Behaviour of Justicia Secunda Leaves Extract as an Eco-Friendly Inhibitor for Aluminium in Acidic Media" 11(2021), 13019 – 13030, doi.org/10.33263/BRIAC115.1301913030

[18] A.I. Ali, Y.S. Mahrousb, "Corrosion inhibition of C-steel in acidic media from fruiting bodies of Melia azedarach L extract and a synergistic Ni2+ additive", RSC Adv. 7(2017) 23687–23698

[19] N.AI Otaibi, H.H. Hammud, Corrosion Inhibition Using Harmal Leaf Extract as an Eco-Friendly Corrosion Inhibitor, Molecules, 26(2021) 7024.https://doi.org/10.3390/molecules26227024

[20] O.O. Adeyemiand, O.O. Olubomehin, "Investigation of Anthocleistadjalonesisstembark extract of corrosion inhibitor for aluminium", Pacific J. Sci. Technol. 11(2010) 455-462.

[21] M. Ismail, A.S. Abdulrahman, M.S.Hussain, "Solid waste as environmental benign corrosion inhibitors in acid medium", Int. J. Engg. Sci. Technol. 3(2) (2011) 1742-1748.

[22] E.F. Olasehinde, S.J. Olusegun, A.S. Adesina, S.A. Omogbehin, H. Momoh- Yahayah, "Inhibitory action of Nicotianatobacumextracts on the corrosion of mild steel in HCl: adsorption and thermodynamic study", Natural Science. 11(2013), 83-90

[23] N. J. Maduelosi and N.B. Iroha, "Insight into the Adsorptive Inhibitive effect of Spironolactone Drug on C38 Carbon Steel Corrosion in Hydrochloric Acid Environment", Journal of Bio and Tribo-Corrosion, 7(2021), doi.org/10.1007/s40735-020-00441-z

[24] N.O. Eddy and A.S. Ekop, "Inhibition of corrosion of zinc in 0.1M H2SO4 by 5-amino-1-cyclopropyl-7-[(3r,5s) 3, 5-dimethylpiperazin-1-yl]-6,8-difluoro-4-oxoquinolne-3-carboxylic acid", Material Science AIJ 4(2007), 2008-2016.

[25] S.Kim, P.A. Thiessen, E.E. Bolton, J. Chen, G. Fu, A. Gindulyte, L. Han, J. He, S.He, B.A. Shoemaker, and J. Wang, substance and compound databases. Nucleic acids research, PubChem 44(2016), .D1202-D1213.

[26] Z.Z.H. Zhenli, "The Computation Basis of Software CS Chem3D and its Application in Organic Chemistry", Guang Zhou Chemical Industry and Technology, 2(2002).

[27] R. Dennington, T.A. Keith, and J.M. Millam, "GaussView 6.0. 16, Shawnee Mission 2016.

[28] M.J. Frisch, G.W. Trucks, H.B. Schlegel, G.E. Scuseria, M.A. Robb, J.R. Cheeseman, G. Scalmani, V. Barone, G.A. Petersson, H. Nakatsuji, and X. Li, Gaussian 16, 2016.

[29] F.J. Devlin, J.W. Finley, P.J. Stephens, and M.J. Frisch, "Ab initio calculation of vibrational absorption and circular dichroism spectra using density functional force fields: a comparison of local, nonlocal, and hybrid density functionals". The Journal of Physical Chemistry, 99(1995), 16883-16902.

[30] R.K. Roy, S. Krishnamurti, P. Geerlings, and S. Pal, "Local softness and hardness-based reactivity descriptors for predicting intra-and intermolecular reactivity sequences: carbonyl compounds", The Journal of Physical Chemistry A, 102(1998), 3746-3755.

[31] I.B. Obot, D.D. Macdonald, and Z.M. Gasem, "Density functional theory (DFT) as a powerful tool for designing new organic corrosion inhibitors. Part 1: an overview. Corrosion Science, 99(2015), 1-30.

Citation: *Godwin Abawulo Ijuo et al."Experimental and Computational Investigation of Anticorrosion Properties of Eastern Nigerian Propolis Extract on Mild Steel in Acidic Medium", International Journal of Advanced Research in Chemical Science (IJARCS), vol. 10, no12, pp. 1-13, 2023. http://dx.doi.org/ 10.20431/ 2455-7153.1001001*